Physical restrictions of the flotation of fine particles and ways to overcome them

Stoyan I. Karakashev [1], **Nikolay A. Grozev** [1], **Orhan Ozdemir** [2], **Onur Guven** [3], **Seher Ata** [4], **Ghislain Bournival** [4], **Khandjamts Batjargal** [2], **Feridun Boylu** [5], **Svetlana Hristova** [6], **Mehmet Sabri Çelik** [5,7]

[1] Department of Physical Chemistry, Sofia University,1 James Bourchier Blvd, Sofia 1164, Bulgaria

[2] Istanbul University-Cerrahpaşa, Mining Engineering Department, Buyukcekmece, Istanbul, Turkey

[3] Adana Alparslan Türkeş Science and Technology University, Mining Engineering Department, Sarıçam, Adana, Turkey

[4] School of Minerals and Energy Resources Engineering, University of New South Wales, Sydney, New South Wales, 2052, Australia

[5] Istanbul Technical University, Mineral Processing Engineering Department, Maslak, Istanbul, Turkey;

[6] Department of Medical Physics and Biophysics, Medical Faculty, Medical University–Sofia, Zdrave Str. 2, Sofia, 1431, Bulgaria

[7] Rectorate, Harran University, Şanlıurfa, Turkey

Corresponding author: fhsk@chem.uni-sofia.bg (Stoyan Karakashev)

Abstract: This work analyses the basic problems of the fine particles flotation and suggests new ways to overcome them. It is well accepted that the poor recovery of fine particles is due to the small collision rate between them and the bubbles due to the significant difference between their sizes. This common opinion is based on a theory, assuming in its first version a laminar regime, but later has been advanced to intermediate turbulence. It accepts that the particles are driven by the streamlines near the bubbles. In reality, the high turbulence in the flotation cells causes myriads of eddies with different sizes and speeds of the rotation driving both bubbles and particles. Yet, a theory accounting for high turbulence exists and states that the collision rate could be much higher. Therefore, we assumed that the problem consists of the low attachment efficiency of the fine particles. Basically, two problems could exist (i) to form a three-phase contact line (*TPCL*) the fine particle should achieve a certain minimal penetration into the bubble, requiring sufficient push force; (ii) a thin wetting film between the bubble and the particle forms, thus increasing the hydrodynamic resistance between them and making the induction time larger than the collision time. We assumed particles with contact angle $\theta = 80°$, and established a lower size flotation limit of the particles depending mostly on the size of the bubbles, with which they collide. It spans in the range of $R_p = 0.16$ μm to $R_p = 0.40$ μm corresponding to bubbles size range of $R_b = 50$ μm to $R_b = 1000$ μm. Hence, thermodynamically the particle size fraction in the range of $R_p = 0.2$ μm to $R_p = 2$ μm are permitted to float but with small flotation rate due to the small difference between the total push force and maximal resistance force for formation of *TPCL*. The larger particles approach slowly the bubbles, thus exceeding the collision time. Therefore, most possibly the cavitation of the dissolved gas is the reason for their attachment to the bubbles. To help fine particles float better, the electrostatic attraction between bubbles and particles occurred and achieved about 92% recovery of fine silica particles for about 100 sec. The procedure increased moderately their hydrophobicity from $\theta \approx 27.4°$ to $\theta \approx 54.5°$. Electrostatic attraction between bubbles and particles with practically no increase of the hydrophobicity of the silica particles ended in 47% recovery. All this is an indication of the high collision rate of the fine particles with the bubbles. Consequently, both, an increase in the hydrophobicity and the electrostatic attraction between particles and bubbles are key for good fine particle flotation. In addition, it was shown experimentally that the capillary pressure during collision affected significantly the attachment efficiency of the particles to the bubbles.

1. Introduction

The collision rate between the bubbles and the particles is important for the high flotation recovery. The calculation of this rate is an old problem. The simplest way to calculate it is by accounting for the streamlines of the fluid carrying a particle in close proximity to a bubble (Von Smoluchowski 1917, Sutherland 1948). This approach has been studied in details (Michael and Norey 1969, Flint and Howarth 1971) and advanced for larger Stokes and Reynolds numbers (Dobby and Finch 1987, Yoon and Luttrell 1989), but up to a certain intermediate level (up to Re = 400) of turbulence, because the general assumption (flow around a bubble) is the same. There is turbulence in the flotation cells in reality. The particles (solid particles and bubbles) are carried out by eddies interacting with each other, hence making them collide (Abrahamson 1975). The size and the speed of rotation of these eddies depend on the Reynolds number. An important factor here is if the particles are bigger or smaller than the smallest eddies and the level of independence of the solid particles from the fluid motion (the Stokes number) (Saffman and Turner 1956, Panchev 1971). For example, the bubbles and the fine particles follow completely the fluid motion, but at very high turbulence the rate of collision is based on Brownian motion (Levich 1962) and the gas kinetic model, thus following the normal distribution of the particles on their velocities (Batchelor 1956). As far as the particles and the bubbles are subjected to random forces, their mean square velocity is the main factor of their random motion (Batchelor 1956). The problem has been treated in detail by several authors (Friedlander 1957, Levins and Glastonbury 1972, Komasawa, Kuboi et al. 1974). They considered that (i) the Eulerian and the Lagrangian coordinate systems are identical for both big and small particles; (ii) the rate of change of particle momentum is equated to: (a) the viscous drag; (b) pressure force; (c) fluid mass entrained with the particles; and (d) history term called the Basset integral. Solution for a steady sinusoidal motion of the fluid has been found along with the probability distribution of the speeds of the particles in one direction (Levins and Glastonbury 1972). Abrahamson (Abrahamson 1975) considered it obtained equations on the rate of collisions between particles of two different types. For example, collision under a constant force field is:

$$Z_{12} = N_1 N_2 \pi d_{12}^2 (W_{t1} - W_{t2}) \tag{1}$$

where N_1 and N_2 are the bulk concentrations of particles of types 1 and 2 (e.g. fine particles and bubbles), d_{12} is the sum of their radii, and W_{t1} and W_{t2} are their terminal velocities. If one assumes 10 µm particles and 200 µm bubbles they should have a very small difference in their terminal velocities because the bubbles are massless while the fine particles have very low mass. Let's assume roughly that this difference is 1 mm/sec and there are 1 wt.% quartz particles and the concentration of the bubbles is the same. Therefore, it will be 9.18x10⁷ particles/m³ and the same concentration of bubbles. Therefore, according to Eq. (1) the rate of collisions between bubbles and particles will be 1.16x10⁶ collisions/sec/m³. Therefore, if all of the collisions are effective, then 80 sec should be enough for all of the particles to be floated with 100% flotation recovery. Of course, this is a rough estimation and the relative difference between the two terminal velocities could be much higher at high turbulence, which could result even in 100% flotation recovery for less than a second if all of the collisions are effective. An important criterion for the lowest radius of the particles, supposed to move completely independent during their collision is given by Abrahamson (Abrahamson 1975):

$$d_p^2 = \frac{15\mu \overline{U^2}}{\rho_p \varepsilon} \tag{2}$$

If one considers quartz particles and the numbers (ε = 4000 W/kg, $\overline{U^2}$= 4 m²/sec²) from ref. (Abrahamson 1975) he will calculate the lower limit of about 76 µm radii of the particles. Therefore, particles with radii above the lower limit move independently toward each other at a high level of turbulence. Therefore, the difference in their terminal velocities can be large, thus resulting in a very high collision rate. The smaller the size of the particles below this lowest size level the more the speeds of the particles are dependent on each other and the difference in their terminal velocity reduces. Moreover, there is a minimum collision rate at a certain critical particle size according to the literature (Reay and Ratcliff 1973), below which the particles (ultrafine) collide with the bubbles under the Brownian regime, while above which they (large particles) collide by means of interception (under hydrodynamic regime). Eq. (2) regards the hydrodynamic regime. There still no real information about the difference in the terminal velocity in the different cases. The calculation of Abrahamson of the rate

of collision between fine particles of two different types in cyclone under high turbulence (ε = 4000 W/kg) operating with real experimental numbers is in the range of 10^{11} collisions/sec/m³. This is a very high number, which results in an instant 100% flotation recovery if all of the collisions are effective. In any case, the fine particles should float with 100% flotation recovery in the time range from part of the seconds to let's say 100 sec if all of the collisions are effective. Experimental data (Ahmed and Jameson 1985) on the flotation of silica particles in the range of radii 5 µm to 20 µm and mean bubble radius in the range of 37 µm to 327 µm and under different impeller speeds report that flotation rate constant: (i) decreases with the decrease of the particle sizes; (ii) increases with the decrease of the bubble sizes; (iii) increases with the increase of the impeller speed. This is in line with the literature data of many other authors, e.g. (De Vivo and Karger 1970, Reay and Ratcliff 1975, Trahar 1976, Anfruns and Kitchener 1977, Trahar 1981, Feng and Aldrich 1999). Physically two factors are important: (**i**) the collision rate between bubbles and particles; (**ii**) the efficiency of collisions between them. Evidently the collision rate should depend on the size of the bubbles, their concentration and the speed of the impeller. The scenario of collision between a bubble and a particle has been studied by number of authors (Sutherland 1948, Philippoff 1952, Dobby and Finch 1986, Yoon and Luttrell 1989, Dai, Fornasiero et al. 1999), thus introducing the contact time as the time of sliding of the particle on the bubble after which the particle retracts from the bubble. Another important parameter is the induction time (often called attachment time) defined as the time, that the bubble needs to capture the particle. If the induction time is smaller than the contact time the bubble captures the particle and vice versa. Theoretical estimation shows that the contact time is in order of milliseconds. An excellent review of Schubert (Schubert 1999) reminds us that the correct approach to the bubble–particle collision should be the one of Abrahamson (Abrahamson 1975) due to the high turbulence during flotation. Therefore, he derived a more precise equation for the rate of collision between particles and bubbles under high turbulence:

$$Z_{BP} = 5N_P N_B d_{BP}^2 \sqrt{\overline{v_p^2} + \overline{v_B^2}} \qquad (3)$$

where N_P and the N_B are the number concentrations of bubbles and particles, $d_{PB} = (d_P + d_B)/2$ and $\overline{v_p^2}$ and $\overline{v_B^2}$ are the root-mean-square values of the turbulent velocity fluctuations of the particles and bubbles, respectively, relative to the turbulent fluid velocity. The latter can be approximately calculated by means of the following equation (Schubert, Heidenreich et al. 1990):

$$\sqrt{\overline{v_i^2}} \approx 0.33 \frac{\varepsilon^{4/9} d_i^{7/9}}{v^{1/3}} \left(\frac{\rho_p - \rho_w}{\rho_w}\right)^{2/3} \qquad (4)$$

where d_i is the diameter of species "i" (bubble or particle), υ is kinematic viscosity, ε is energy dissipation rate, ρ_p is the density of the particle's mineral, ρ_w is the density of water. If the parameters are considered for Eq. (1) and ε = 4000 W/kg (high turbulence) and use Eqs. (3) and (4), it can be calculated that the rate of collision between bubbles and particles is 7.66×10^9 collisions/sec/m³. At this very high rate of collision between the bubbles and the fine particles, all the fine particles should be floated for only 0.012 sec if all of the collisions are effective. An excellent review on the collision models can be found in ref. (Meyer and Deglon 2011). It addresses the development of the collision theory for a period of 100 years starting from collisions in laminar fluid (small Stokes numbers) to collisions in turbulent flows under various additional assumptions. Overall, two approaches exist: (**i**) the approach of von Smoluchowski (Von Smoluchowski 1917), later advanced by many authors but valid up to a certain intermediate turbulence level; (**ii**) the approach of Abrahamson (Abrahamson 1975), which is valid for high turbulence and inertias particles (and later advanced). Both approaches are recognized in the literature, but unfortunately, when they are applied to fine particles they give controversial results. The approach of Abrahamson gives a high collision rate while the approach of Von Smoluchowski gives a low collision rate. As far as the flotation occurs at high turbulence this approach of Abrahamson is more justified. Therefore, there is a high collision rate between bubbles and fine particles under high turbulence, but the collection efficiency of the fine particles are small (Ahmed and Jameson 1985, Ralston, Fornasiero et al. 2007, Manouchehri and Farrokhpay 2016, Fornasiero and Filippov 2017). These works and many others report a decrease in the recovery with the decrease of the size of the particles and an increase of the recovery with the decrease of the size of the bubbles. Of course, mixture of small and the big bubbles works by means of turbulent micro-flotation (Rulyov 2001, Ahmadi, Khodadadi et

al. 2014, Calgaroto, Azevedo et al. 2015, Rulyov, Tussupbayev et al. 2015) as far as the small bubbles have small rising velocity. If Eqs. (3) and (4) are used to impose a radius of the bubbles 20 μm, it will be calculated $Z_{PB} = 3 \times 10^7$ collisions/sec/m^3. This means that the above-mentioned 1 wt.% suspension of fine silica particles should be floated completely for only 3 sec if all of the collisions are effective. Refs. (Pease, Curry et al. 2005, Pease, Young et al. 2010) report signicant increase of the recovery of sphalerite fines by additional grinding and cleaning of the thus obtained fines, but to our knowledge this method has not been proved to work for other ores. A very nice review on the fine partile flotation can be found in ref. (Farrokhpay, Filippov et al. 2020). It sugggests ways to overcome the proble, by aggregation of the fine particles, introducing of micro-bubbles into the flotation cell and designing of special reactor – separator increasing the turbulence. A number of cell with intensified turbulence were suggested to increase the fine particles recovery(Hassanzadeh, Safari et al. 2022). Hence, the problem with the fine particle flotation is not in the rate of the collision with the bubbles but in the efficiency of these collisions.

2. Theoretical analysis of the particle–bubble interaction

The above-mentioned review of the literature shows that the bubbles and fine particles collide at a sufficient rate under high turbulence. Therefore, the problem must be hidden in the efficiency of their collision. The study by Ahmed and Jameson (1985) will be used as an example study (Ahmed and Jameson 1985). Fig. 1 shows the flotation rate constants of silica particles with different sizes at different bubble sizes and different speeds of the impeller (Ahmed and Jameson 1985). One can see in that the flotation rate constant is: (i) proportional to the particle size; (ii) inversely proportional to the bubble size; (iii) is proportional to the impeller speed but the very dependence looks complicated. There are many other studies in the literature about the effect of the above-mentioned factors on the flotation recovery of particles of different sizes. All of them are consistent and agree with Fig. 1. To treat the problem in more detail a theoretical analysis of the bubble–particle interaction was made. Generally, the induction time should be shorter than the collision time for the successful capture of the particle by the bubble. Therefore, the processes occurring during this induction time are important. An interaction between particle and bubble can be observed in a straight collision between them (no sliding). When a particle, pushed by a random turbulent force, approaches a bubble a thin wetting film emerges, thus creating significant hydrodynamic resistance, which decreases the speed of approach. This hydrodynamic interaction deforms the "contact area" of the bubble, thus turning on the capillary additional force pushing the particle toward the bubble. Finally, the particle penetrates the bubble in its "contact area" but is still being separated from the bubble by the thin wetting film. If the penetration is sufficient the film ruptures and a three-phase contact line (*TPCL*) forms on the particle, which allows the bubble to hold and carry the particle. The most important phenomenon here is the rupturing of the wetting film and the formation of *TPCL*. Therefore, it will first fix the attention on this process.
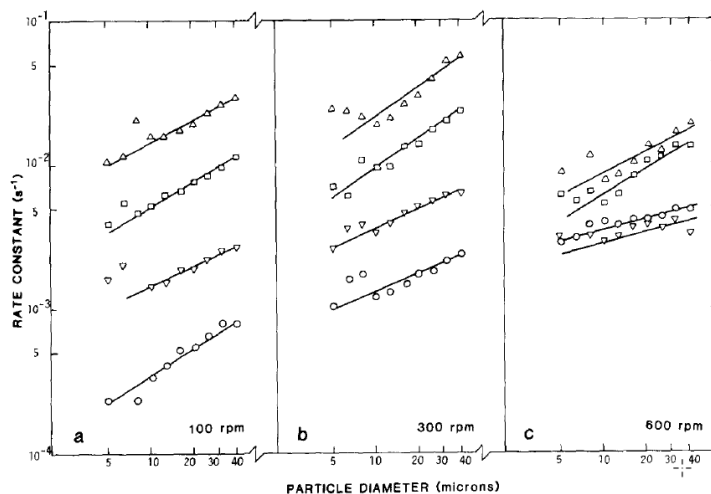

Fig. 1. The flotation rate constant of silica particles is plotted as a function of particle diameter, for the stirrer speeds and bubble diameter shown. Bubble size: $\triangle$ = 75 μm; $\square$ = 165 μm; ∇ = 360 μm; $\bigcirc$ = 655 μm. Printed with the permission of Elsevier with License No 5331211183811 and taken from (Ahmed and Jameson 1985)

2.1. Capillary theory for the formation of *TPCL* on a spherical particle in contact with a bubble

The capillary theory of flotation by Scheludko et al. (Scheludko, Toshev et al. 1976) can be used to make the particular analysis of the requirements for the formation of the *TPCL* on the surface of the particle. Fig. 2 shows a drawing of a spherical particle with radius *R* entering a bubble, thus forming *TPCL* with radius *r*. The central angle α, which defines the position of the particle with respect to the undisturbed surface of the bubble, is also the angle between the center of the particle and the radius of the *TPCL*. The angle β is the angle between the tangent of the sphere with the respect to the radius of the particle at the point of the *TPCL* and the vertical line and θ_R is the contact angle of the spherical particle at the point of the *TPCL*.
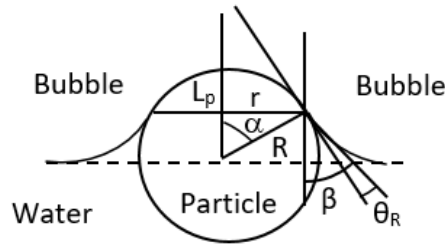

Fig. 2. *TPCL* on a spherical particle that enters a bubble from the aqueous phase

The Young equation for a spherical particle penetrating a bubble and already formed *TPCL* with radius *r* is and line tension *k* (Scheludko, Toshev et al. 1976):

$$\sigma_{S/A} - \sigma_{S/L} = \sigma_{A/L}\cos\theta_R - \frac{k}{r}\cos\alpha \tag{5}$$

The contact angle θ_R regards only the spherical particle and it is different from the contact angle θ, which is the contact angle of a small aqueous droplet on a flat surface from the same material as the particle. The latter obeys the classical Young equation

$$\cos\theta = \frac{\sigma_{S/A} - \sigma_{S/L}}{\sigma_{L/A}} \tag{6}$$

Hence, Eq. (5) can be presented as:

$$\cos\theta_R - \cos\theta = \frac{k}{\sigma_{A/L}r}\cos\alpha \tag{7}$$

TPCL cannot be formed when $\theta_R = 0°$ because this corresponds to the complete wetting of the particle by the water. One can be seen in Fig. 2 and Eq. (7) that the angle θ_R is a function of the angle α, which depends on the level of penetration of the particle into the bubble prior to rupturing of the wetting film, hence, from $\alpha = 0°$, (no penetration) to $\alpha = \alpha_c$ (critical level of penetration), $\theta_R = 0°$ and consequently, *TPCL* cannot form spontaneously. *TPCL* forms spontaneously $\alpha > \alpha_c$. Therefore, it is assumed $\theta_R = 0°$, and $\alpha = \alpha_c$ and $r = R\sin\alpha_c$ in Eq. (7) and obtain:

$$tg\,\alpha_c = \frac{k}{R\sigma_{A/L}(1-\cos\theta)} \tag{8}$$

There is a resistance force for the formation of *TPCL*, supposed to be overcome by the pushing force:

$$f = 2\pi r\sigma\cos\beta \tag{9}$$

With $\beta = \pi/2 - \alpha$ and $r = R\sin\alpha$ one obtains:

$$f = 2\pi R\sigma\sin^2\alpha \tag{10}$$

Therefore, at $\alpha = \alpha_c$, there is maximal resistance force $f = f_c$ and the combination of Eqs. (8) and (10) gives:

$$f_c = \frac{2\pi R\sigma_{L/A}}{1+\left[\frac{R\sigma_{L/A}}{k}(1-\cos\theta)\right]^2} \tag{11}$$

If silica particle (ρ = 2600 kg/m³) with radii in the range of 0.1 μm to 100 μm and speed of 0.1 m/sec and collision time of 1 ms are considered, the pushing force of the particle toward the bubble versus its radius can be calculated. At the same time, Eq. (11) gives the maximal resistance force for the formation of *TPCL* versus the radius of the particle. It was assumed $\theta = 80°$. There is a second push force except for the random one – the capillary force, which will be described in the next subsection. The sum of both

push forces gives the total push force. The total push force and the resistance force for the formation of *TPCL* are presented in Fig. 5.

2.2. Drainage of thin wetting film between a spherical particle and bubble

Another important factor for consideration is the time of drainage of the wetting film between the particle and the bubble because it is related to the induction time. Therefore, as a criterion, the drainage of the wetting film was considered from the distance of 1 μm to 0.02 μm. The particle is subjected to hydrodynamic pushing force F_{zh} when it is approaching the bubble. When both of them interact hydrodynamically the bubble in its contact area deforms, thus gradually adjusting its shape to the shape of the particle. This reshaping of the contact area of the bubble generates additional capillary pushing force F_{zc}. For simplicity, it could be assumed that a planar film with a radius equal to the radius of the particle is formed ($R_f = R_p$). It must be confessed that this solution is approximate, but it is not expected more than a 10% deviation from the precise solution. Therefore, the Reynolds law can be used for the drainage of thin wetting film between planar air/liquid and solid/liquid interface (Slavchov, Radoev et al. 2005, Karakashev, Stoeckelhuber et al. 2011):

$$V \frac{8F_z}{3\pi\mu R_f^4} \quad^3_{Re}$$

(12)

Where F_z is the pushing force of the particle towards the bubble ($F_z = F_{zh} + F_{zc}$), μ is the dynamic viscosity of the water, R_f is the radius of the wetting film, and h is the thickness of the wetting film, which is the distance between the particle and the contact area of the bubble. For simplicity, the effect of the disjoining pressures can be neglected, but only the hydrodynamic random and the capillary forces can be considered. This can be justified if the ionic strength is larger than 0.01 mol/dm³ (screened electrostatic interaction) and the van der Waals interaction becomes significant at a thickness less than 10 nm. As far as a planar wetting film the capillary force can be presented by:

$$F_{zc} = \frac{2\sigma_{A/L}}{R_b}\pi R_f^2$$
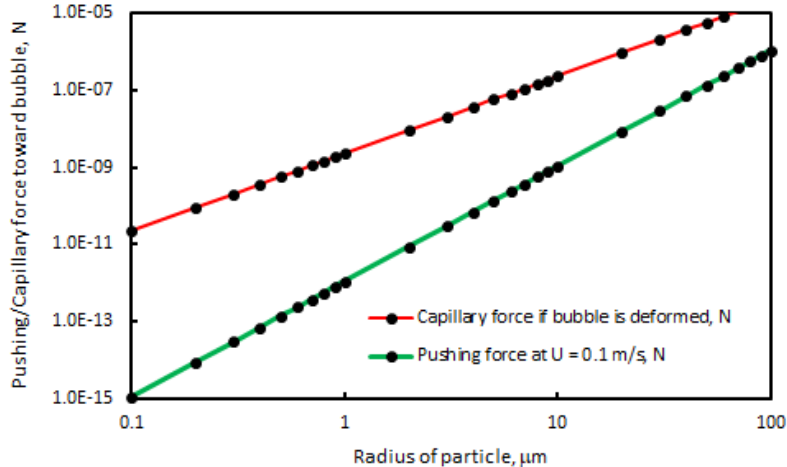
(13)

Fig. 3. Capillary and pushing forces versus radius of silica particle moving with 0.1 m/sec toward a bubble with a radius of 200 μm

The pushing force is a very important factor. Therefore, again it should be accepted silica particles with radii in the range of 0.1 μm to 100 μm moving with a speed of 0.1 m/sec and collision time of 1 ms. It is also assumed as well bubbles with a radius R_b = 200 μm. Fig. 3 presents the capillary and the pushing forces versus the radius of the particle. One can see in Fig. 3 that both forces are proportional to the size of the particle and the capillary force is larger in magnitude than the pushing force. This indicates the importance of the capillary pressure during the bubble–particle interaction. As far as the drainage of the wetting film is related to the induction time, the time of drainage of the wetting film on the same bubbles was calculated from the distance of 1 μm to 0.02 μm versus the radius of the particles, as shown in Fig. 4.

It must be reminded that all the particles deform the bubble in its contact area during their straightforward collision, so the capillary pressure is accounted for in the calculation. One can see in Fig. 4 that the fine particles approach the bubble very fast due to the small area of their wetting films, while the bigger particles approach the bubble significantly slower due to the larger area of their wetting films. It is curious to see that this time of drainage significantly exceeds the collision time in the real flotation (1ms). Therefore, according to Fig. 4 particles with a radius larger than 1 μm should never be captured by the bubbles because they do not have sufficient time to approach the bubble.

On the contrary, the experiment shows that hydrophobized particles of large size are floated very well. How can this controversy be explained between a theory and an experiment? The only reason for the good flotation of large particles could be the cavitation of the dissolved gases during the drainage of the wetting film. If no cavitation occurs the capture of the particle by the bubble is impossible. Fig. 5 shows the total push force and the maximal hydrodynamic force versus the radius of the particles. According to Fig. 5, the lower limit for flotation of fine particles is R_p= 0.24 μm. The lower size limit is weakly dependent on the speed of the particles, but it depends on the size of the bubbles, with which they collide (see Fig. 6).

Therefore, particles with radii larger than the lower size limit, as shown in Fig. 6, can be captured by the bubble. The main question here is the reason for their poor recovery. The basic reason according to us is in the level of exceeding of the total push force over the maximal resistance force for formation of
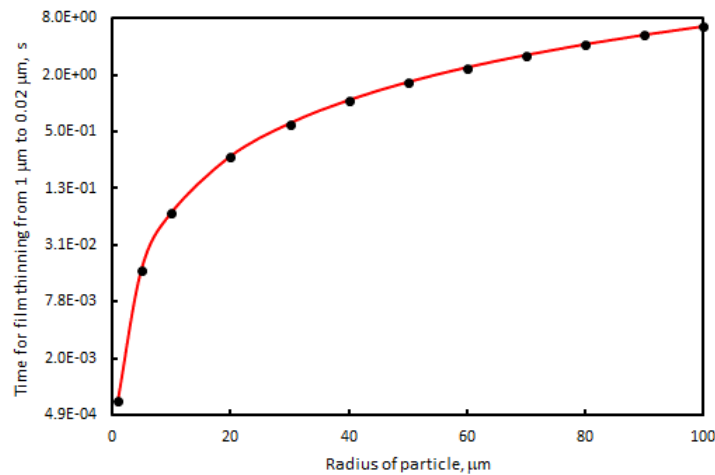

Fig. 4. Time for thinning of a wetting film between a silica particle moving with 0.1 m/sec and a bubble with a radius 200 μm from distance 1 μm to distance 0.02 μm from the contact area of the bubble vs. the radius of the particle
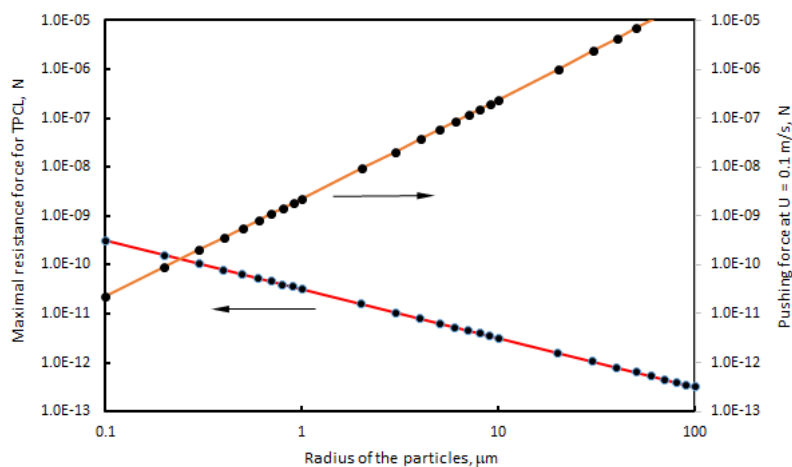

Fig. 5. Maximal resistance force for the formation of *TPCL* and total pushing force (hydrodynamic + capillary ones) of particle toward a bubble as a function of the radius of hydrophobized silica particles with $\theta = 80°$ and moving with 0.1 m/sec
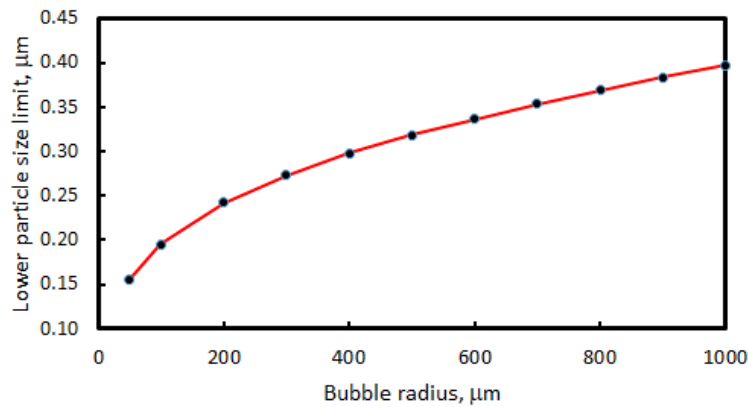
Fig. 6. Lower particle size limit for attachment of particle with contact angle $\theta = 80°$ vs. with a bubble radius R_b

TPCL. This exceeding lies in the range of 0.1 nN to 10 nN for particle radii in the range of $R_p = 0.3$ μm to $R_p = 2$ μm. Evidently this nano-Newton range is insufficient to initiate faster flotation of the fine particles. Just for comparison, in the thin liquid film experiments the driving capillary force is a least 300 nN. So it is not surprise that the floatation of fine particles occurs with small rate. To assemble the whole picture of the bubble–particle interaction projected by both the capillary and the drainage theories it should be concluded that: (**i**) particles with radii in the range of 0.2 μm to 2 μm are floated but with a small rate due to insufficient push force; (**ii**) particles with radii larger than 2 μm should have induction time larger than the contact time; the only reason for their floatability could be the cavitation of dissolved gases. Fig. 7 shows the experimental flotation rate constant versus the radii of hydrophobized silica particles with contact angle $\theta = 80°$ (Pyke, Fornasiero et al. 2003). One can see in Fig. 7 that the cavitation effect increases with the increase of the size of the particles.

   As far as our attention is focused on the fine particles, we could conclude that they need additional push force to increase the level of exceeding of the total push force over the maximal resistance force for formation of *TPCL*.
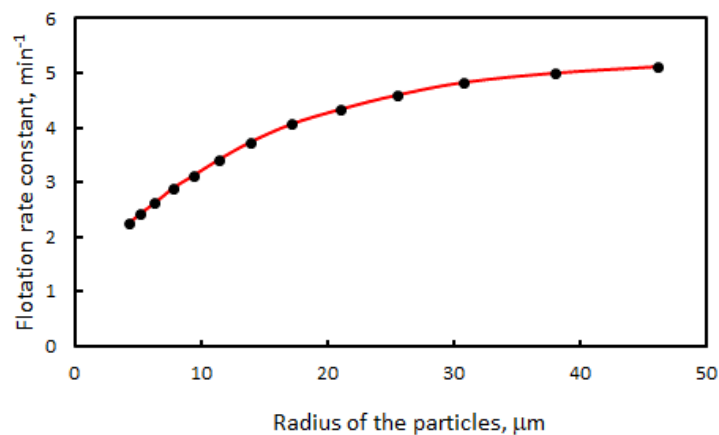

Fig. 7. Flotation rate constant of silica particles with contact angle $\theta = 80°$ vs. the radius of the particles (Pyke, Fornasiero et al. 2003)

3. Materials and methods

3.1. Materials

Hexylamine purchased from Sigma-Aldrich has been used as a collector to modify the quartz plate and the silica particles. The quartz plate has been cut as a square of 2 mm x 2 mm, polished and cleaned with a specially prepared alkaline solution, and rinsed well with deionized (*DI*) water (Milli-Q) prior to the experiment. The silica particles (-10 μm), used in the Hallimond tube, were purchased from Sigma-Aldrich as well. Amino-3-methoxy silane (APTMS) was purchased from Sigma-Aldrich. Sodium

hydroxide and ethanol were purchased from Sigma-Aldrich. Another set of silica particles was provided by Unimin Australia Ltd (Victoria) and was wet sieved to 20 µm and used for the flotation experiments with the Denver flotation machine.

- *Pretreatment with Hextlamine:* the particles/quartz plate was soaked in 0.05 mol/dm³ Hexylamine for 24 hours under intensive stirring, after which they were very well rinsed with *DI* water and dried.
- *Pretreatment with Amino – 3 – methoxy silane (APTMS):* The silica particles were soaked in 1 mol/dm³ NaOH at temperature T= 60° under intensive stirring. After that, they were rinsed very well with *DI* water followed by another soaking in a mixture of 100 mol ethanol + 2 cm³ Amino – 3 – methoxy silane (APTMS) for 24 hours at temperature T= 60°. After that, they were rinsed very well with *DI* water. Shown in Fig. 8 is the basic chemical reaction with the silica particles causing its modification. As seen in Fig. 8 there are amino groups on the chains attached to the silica surface. Due to the latter one, the isoelectric point of the modified silica particles is shifted to pH = 9.2.

Fig. 8. Reaction of amino-3-methoxy silane (APTMS) with the silica surface Si−OH groups

3.2.   Methods

3.2.1. Thin wetting films experiments

An interferometric study was conducted on thin wetting films between a bubble and quartz flat surface by means of the Scheludko-Exerowa cell (Exerowa and Kruglyakov 1997). Shown in Fig. 9 is the interferometric setup of Scheludko-Exerowa (Exerowa and Kruglyakov 1997) adjusted for wetting films on an opaque mineral surface (Karakashev, Stoeckelhuber et al. 2011). The experiment was conducted at a constant room temperature of 20°C. Briefly (see Fig. 9), the apparatus consists of a glass cell, for producing horizontal wetting films, normal to gravity. First, a water droplet was placed inside the film holder. After this, the plate of the mineral (square of 2 mm x 2 mm) was positioned carefully on the top of the cell's holder (see Fig. 9).

After this, some amount of liquid was pumped out by means of a gastight micro-syringe, thus forming a microscopic thin wetting film between the mineral surface and the apex of the water droplet. A metallurgical inverted microscope (model IX 51, Olympus Corporation, Japan) was used for

Fig. 9. Interferometric setup of Scheludko-Exerowa for studying thin wetting films (Karakashev, Stoeckelhuber et al. 2011)

illuminating and observing the film and its interference fringes (the Newton rings) in polychromatic light. The film evolution was captured by a CCD camera connected with a computer and stored as a movie for further processing. The description of the procedure for converting the interferogram into a real film thickness profile is given in detail in the literature. (Karakashev, Stöckelhuber et al. 2013). Films with radii smaller than 50 μm are close planar films. Therefore, one can assume that the wetting film has practically the same thickness. Having this into consideration, one can make a surface force analysis of the wetting film by means of its kinetics of thinning. Films with a small amount of surfactant have usually stagnant surfaces. Therefore, if their radii are enough small their thinning can be described by means of the following equation:

$$-\frac{dh}{dt} = \frac{8h^3}{3\mu R_f^2}(P_\sigma - \Pi) \tag{14}$$

where h is the film thickness, R_f is the film radius, μ is the bulk dynamic viscosity, $P_\sigma = 2\sigma/R$ is the capillary pressure, σ is surface tension, R is the radius of the film holder, and $\Pi = \Pi_{el} + \Pi_{vdW}$ is the total disjoining pressure, which is a sum of the electrostatic Π_{el} and van der Waals Π_{vW} disjoining pressures.

The electrostatic disjoining pressure can be described by the following formula assuming constant surface potentials (valid for foam, emulsion, and wetting films) (Kralchevsky, Danov et al. 2016):

$$\Pi_{el} = \frac{\varepsilon\varepsilon_0\kappa^2}{2\pi}\frac{2\Psi_{s1}\Psi_{s2}\cosh(\kappa h)-(\Psi_{s1}^2+\Psi_{s2}^2)}{\sinh^2(\kappa h)} \tag{15}$$

where ε and ε_0 are the static dielectric permittivities of water and free space, $\kappa = \sqrt{2F^2c_0/\varepsilon\varepsilon_0 R_g T}$ is the Debye constant (in SI unit), F (F = 96 485.33 C/mol) is the Faraday constant, c_0 is the electrolyte concentration (in case of DI water $c_0 = 3.10^{-3} mol/m^3$ due to the dissolved carbon dioxide), R_g is the gas constant and T is temperature, Ψ_{s1} and Ψ_{s2} are the surface potential values of the first (air/water) and the second (water/solid) surfaces, and finally h is wetting film thickness. Eq. (15) is derived for the cases of very different/or opposite surface potentials of the two surfaces of the film. Another equation for the electrostatic disjoining pressure, based on the superposition approximation (Kralchevsky, Danov et al. 2008) and valid for the surfaces with the same sign of the surface potential reads:

$$\Pi_{el} = 64cR_gT\tanh\left(\frac{F\Psi_{s1}}{4R_gT}\right)\tanh\left(\frac{F\Psi_{s2}}{4R_gT}\right)\exp(-\kappa h) \tag{16}$$

The van der Waals disjoining pressure, Π_{vdW}, as a function of the film thickness, h, for both the non-retarded and retarded regimes can be described as (Nguyen and Schulze 2004):

$$\Pi_{vdW} = -\frac{A(h,\kappa)}{6\pi h^3} + \frac{1}{12\pi h^2}\frac{dA(h,\kappa)}{dh} \tag{17}$$

Where $A(h,\kappa)$ is the Hamaker-Lifshitz function, which depends on the film thickness and the Debye constant, κ, due to the electromagnetic retardation effect and is described as:

$$A(h,\kappa)_{132} = \frac{3k_BT}{4}(1+2\kappa h)e^{-2\kappa h} + \frac{3\hbar\omega}{16\sqrt{2}}\frac{(n_1^2-n_3^2)(n_2^2-n_3^2)}{(n_1^2-n_2^2)}\left\{\frac{I_2(h)}{\sqrt{n_2^2+n_3^2}} - \frac{I_1(h)}{\sqrt{n_1^2+n_3^2}}\right\} \tag{18}$$

$$I_j(h) = \left[1 + \left(\frac{h}{\lambda_i}\right)^q\right]^{-\frac{1}{q}} \tag{19}$$

$$\lambda_i = \frac{2\sqrt{2}c}{\omega\pi}\sqrt{\frac{1}{n_3^2(n_i^2+n_3^2)}} \tag{20}$$

where $\hbar$ = 1.055 × 10⁻³⁴ J·s/rad is the Planck constant (divided by 2π), ω is the absorption frequency in the UV region – typically around 2.068 × 10¹⁶ rad/sec for water, n_1, n_2, and n_3 are the characteristic refractive indices of the two dispersion phases (air and mineral) and the medium (water): $n_1^2 = 1$ for air, $n_3^2 = 1.887$ for water, $n_2^2 = 2.28$ for magnesite ($n_2^2 = 2.359$ for crystalline quartz), $c = 3.10^8$ m/s is the speed of light in free space, and $q = 1.185$, λ_1 and λ_2 are characteristic wavelengths of first (air/water) and second (water/solid) surfaces of the wetting film.

3.2.2. Flotation experiments

Two kinds of flotation experiments were conducted: (i) with a Hallimond tube; (ii) with a Denver flotation machine.

- *Hallimond tube:* Suspension of 1 wt.% silica particles preliminary treated, was prepeared and poured into the Hallimond tube. Nitrogen with a rate in the range of 0.2 dm³/min – 0.4 dm³/min was sparged through the bottom of the cell for 2 min. The concentrate was taken during this time. After that concentrate and the tailing were put aside, dried, and weighted.
- *Denver flotation machine*: Graded silica 100 G provided by Unimin Australia Ltd (Victoria) was wet sieved to 20 µm. The undersize fraction was employed for the flotation experiments. The particles were soaked for 24 hours in a 1:10 solution of HCl. The solution was then decanted and the particles were redispersed in *DI* water and decanted again. The process was repeated until the pH of the decanted solution was that of *DI* water. The flotation experiments were conducted in a Denver flotation cell compliant with the Australian Standard for coal flotation (Australian Standard 2016). The flotation cell was approximately 3.5 dm³ and equipped with a deflector block. *DI* water was added to the cell and, with the impeller set at a speed of 1000 rpm, a slurry of 1% w/w solids was produced. Hexylamine was added at a concentration of 0.05 mol/dm³ to the cell and the slurry was conditioned for 10 min. The pH of the slurry was measured at 11.82. During the flotation experiments, the froth depth was maintained at 20 mm and the superficial gas velocity (J_g) was set to 0.5 cm/sec. The scrapping rate of the froth, which is important in the transfer kinetic of particles (Amelunxen, LaDouceur et al. 2018), was one scrape every 5 sec. The products were collected at various times for 240 sec. The concentrates and the tailings were dried in an oven and weighed.

3.2.3. Bubble–particle attachment time measurements

The attachment mechanism of bubble and particle is very important for flotation performance, and clarifying the mechanism is so crucial. While contact angle measurement is a static method, and is widely used to determine the hydrophobicity of particles, bubble-particle attachment time measurement is dynamic, and it gives us the time required for bubble-particle attachment to occur, and it is strongly controlled by the surface chemistry of the mineral and bubble. The bubble attachment time experiments can be carried out in the mineral's natural state or with surfactant addition. Moreover, the results obtained from these measurements are important to understand the flotation behaviour of the minerals due to the strong relation between bubble attachment time measurements and flotation results. The shorter the bubble attachment time, the higher the flotation recovery is. The bubble attachment test is also a unique method to determine the hydrophobicity of minerals. The particle-bubble interaction can be described in three independent steps: (i) a collision between particle and bubble (Step 1), (ii) attachment of the particles to the bubble (Step 2), and (iii) the stability of bubble-particle aggregate (Step 3). A schematic presentation of the proposed bubble attachment time experiments is also shown in Fig. 10 which consists of a force sensor head, a long-distance working lens and CCD camera, a micro-translation stage, an illuminator, and a computer. The interactions between the bubble and particles in flotation systems can be determined based on bubble attachment time (induction time) measurements. Moreover, the physical parameters affecting the bubble attachment time such as particle size, bubble size, pH, temperature, etc. can be studied (Ozdemir, Karaguzel et al. 2009a, Ozdemir, Karakashev et al. 2009b, Gungoren, Ozdemir et al. 2019).
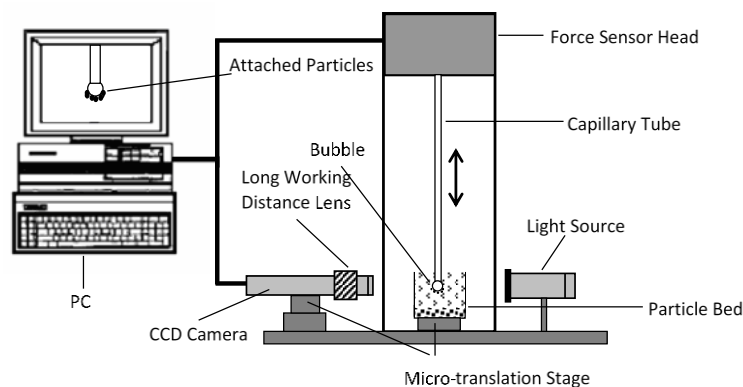

Fig. 10. Schematic presentation of bubble-particle attachment time unit

The main objective of the experiments is to explain the bubble-particle- interactions based on the bubble-particle attachment time values. As well-known, the efficiency of flotation is strongly related to the collecting ability of air bubbles. The time required for bubble-particle attachment has a crucial role and is controlled by the physicochemical properties of both bubble and particles. Besides other static methods, "bubble-particle attachment time" measurement is a dynamic method that provides the minimum time required for bubble-particle attachment to occur. This relation may be defined in three independent steps as described above. Bubble-particle attachment time measurements were carried out with BCT-100 (Bratton Engineering and Technical Associates, LLC, USA) bubble-particle attachment time measurement unit. In these experiments, it is possible to create bubbles of different sizes using capillary which provides a size of about 2, 1, and 0.5 mm. For the measurements, a bubble with a 2 mm radius is first created using a micro-syringe, then the distance between the bubble and the particle bed is adjusted. Following this step, the bubble is contacted with the bed surface and held within the given time (ms). Then, the bubble is replaced, and the adhering particles on the bubble surface are observed. This process is repeated at least 20 times in different parts of the particle bed and the observations are recorded. After the measurements, the observations are converted to graphs, and the time needed for 50% attachment time is determined as the bubble-particle attachment time (Albijanic, Ozdemir et al. 2010).

4.   Results and discussion

4.1. Thin wetting films

It can be focused mostly on the electrostatic and van der Waals interaction between the bubble and a plate of quartz. The zeta potential of air bubbles in the *DI* water is about $\zeta \approx -$ 65 mV ± 12 mV (Karakashev, Firouzi et al. 2019), and its isoelectric point is pH $\approx$ 4. Therefore, an air bubble in *DI* water has surface potential $\Psi_s \approx -$ 65 mV (pH = 5.8), while at pH = 4, $\Psi_s \approx$ 0 mV. Let's see how a wetting film from DI water will behave on a quartz surface. The kinetics of thinning of wetting film on quartz surface in DI water is presented in Fig. 11. The dots present the experimental data, while the red line presents the theoretical curve according to Eq.(14)). One can see that the wetting film gets into equilibrium at about 150 nm, which corresponds to strong repulsion with the surface potential of the quartz $\Psi_s \approx -$ 90 mV. The latter one is the only unknown parameter in the equation and it was calculated following the *DLVO* theory. The *DLVO* analysis on bubble-approaching quartz surface in *DI* water is presented in Fig.12. As seen in Fig. 12, there are two repulsive disjoining pressures – the electrostatic one and the van der Waals one. Both disjoining pressures are summed in total disjoining pressure. Therefore, when the total repulsive disjoining pressure becomes equal to the "squeezing" capillary pressure, which pushes the film to thin, the film gets into equilibrium and does not drain anymore. For thisr particular case, this happens at about 150 nm (see Fig.12). These equilibrium films can last for many minutes and hours.

Let's now see what will be the behavior of wetting film on quartz at the isoelectric point of the bubble (pH = 4), i.e. its surface potential is equal to zero mV. Therefore, it should not be any electrostatic repulsion between the bubble and the quartz surface, but only dispersion repulsion between them should exist. The drainage of such a wetting film, but in presence of 10^{-4} mol/dm^3 MIBC ($\approx$ *CCC*) is

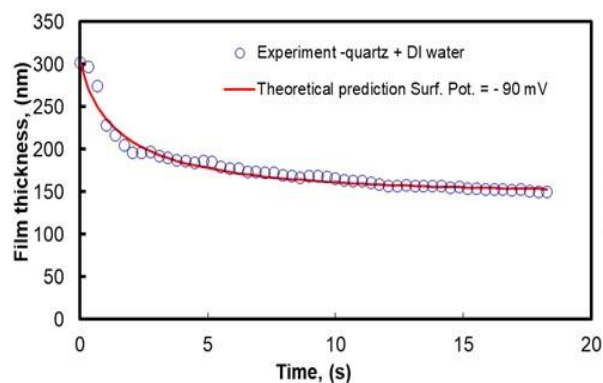Fig. 11. Wetting film thickness versus time on quartz in *DI* water (pH = 5.8): dots – experimental curve, the red line is the theoretical curve (Eq.(14))
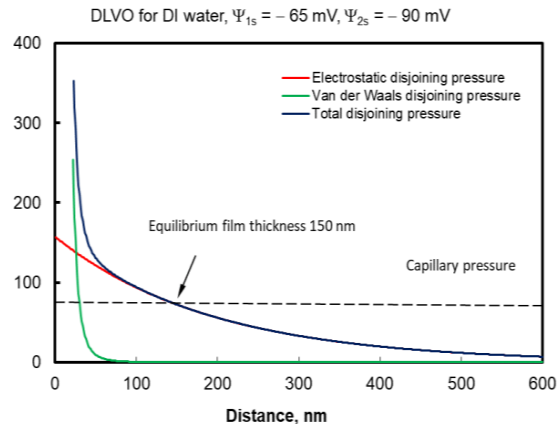
Fig. 12. Electrostatic, van der Waals, and total disjoining pressure between a bubble and a quartz surface in *DI* water (pH = 5.8) versus distance between them

presented in Fig. 13. No electrostatic repulsion was exist in the theoretical Eq. (16), but only accounted for the van der Waals repulsion (Eqs.(17)-(20)).

One can see an acceptable coincidence between theory and experiment. The film thinned until about 30 nm, where it got into equilibrium, due to the van der Waals repulsion between the quartz surface and the bubble. The *DLVO* analysis in Fig. 13 is presented in Fig. 14. One can see no electrostatic repulsion between the bubble and the quartz surface. The total and the van der Waals disjoining pressures coincide, thus becoming equal to the capillary pressure at about 30 nm, which is the equilibrium film thickness.

The quartz surface was treated with hexylamine $C_6H_{13}NH_2$. The latter one hydrolyzes in water making its pH value very alkaline (pH = 11.2):

$$C_6H_{13}NH_2 + H_2O \rightarrow C_6H_{13}NH_3^+ + OH^- \tag{21}$$

Therefore, the surface-active cations should adsorb on both the quartz surface and the bubbles. The quartz surface was treated in the following way: it was cleaned with acetone and ethanol and rubbed very well with special tissue.

After this, it was immersed in 0.05 mol/dm³ aqueous solution of hexylamine for 24 hours under intensive stirring with a magnetic bar. Then, it was pulled out and flushed well with *DI* water and dried. Thus, the plate was positioned on the film holder and wetting film of *DI* water was formed on it in the way described above. It was firstly choosen to study wetting film treated with hexylamine quartz surface in *DI* water, just to check if the electrostatic attraction is realized. If the wetting films are in a medium of 0.05 mol/dm³ hexylamine, the electrostatic interaction will be screened completely because the inverted Debye length of the 0.05 mol/dm³ electrolyte is $1/\kappa$ = 1.36 nm. Shown in Fig. 15 is the film thickness versus the time of wetting film on treated with hexylamine quartz in *DI* water. The dots present the experimental data, the red line is a theoretical curve with no electrostatic repulsion and the
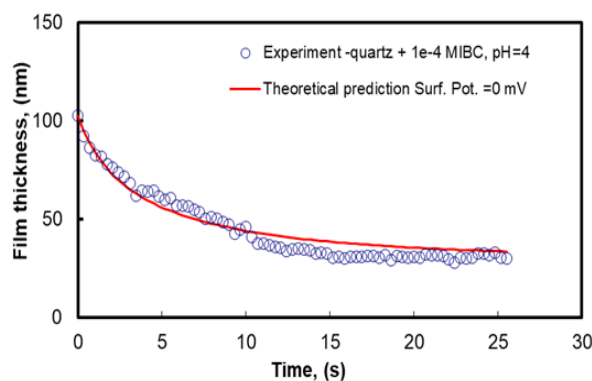

Fig. 13. Wetting film thickness versus time on quartz in 10^{-4} mol/dm³ MIBC at pH = 4: dots – experimental curve, the red line is the theoretical curve (Eq.(14))
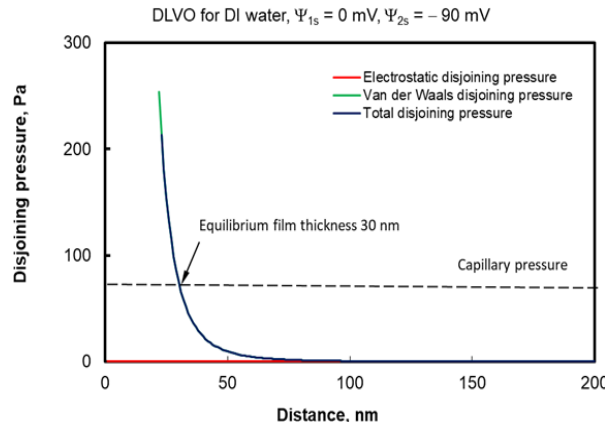
Fig. 14. Electrostatic, van der Waals, and total disjoining pressure between a bubble and a quartz surface in 10^{-4} mol/dm³ MIBC (pH = 4) versus distance between them
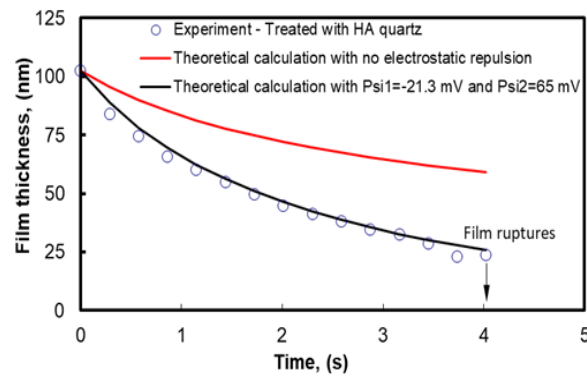

Fig. 15. Wetting film thickness versus time on modified with hexylamine (HA) quartz in *DI* water: dots are the experimental curve, the red line is the theoretical curve with excluded electrostatic repulsion (Eq.(14)), while the black line is the theoretical curve
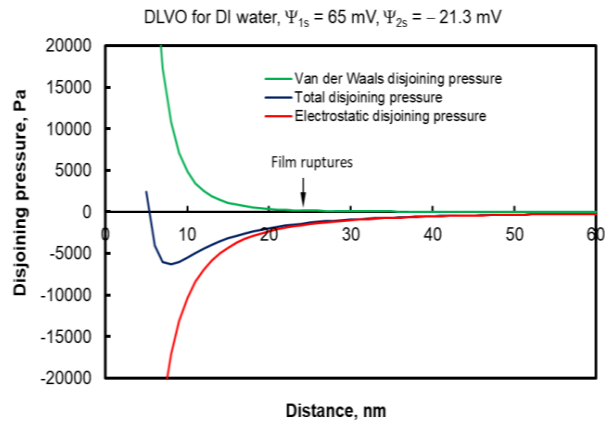

Fig. 16. Electrostatic, van der Waals, and total disjoining pressure between a bubble and a treated with hexylamine quartz surface in *DI* water

black line is the theoretical curve with a surface potential of the quartz surface $\Psi_s = -21.3$ mV and surface potential of the air/water interface $\Psi_s = 65$ mV. One can see that the wetting film drains faster than the predicted by the theory of drainage with no electrostatic repulsion. This means that there is an additional attraction between the film surfaces, which could be only an electrostatic one. Moreover, to evaluate how strong is this attraction Eq. (15) should be used, which has been derived (Kralchevsky, Danov et al. 2016) for cases of very different or oppositely charged surfaces.

Yet, to use this equation there needs to know the surface potentials of the quartz surface and the one of the bubble. For this reason, the zeta potential values of STERILES – MS 45 gangue mineral particles versus pH were measured. They contain 41.22% SiO_2. Therefore, the application of Eq.(14), (15), and (17) utilizing the fitting procedure on the experimental points ended in the surface potential of the bubbles Ψ_s = 65 mV. The *DLVO* analysis in Fig. 15 is presented in Fig. 16. One can see that the total disjoining pressure is negative until about 6 nm, which corresponds to attraction, which increases gradually until a thickness of 8 nm, thus forming a potential well. The film ruptured at a thickness of about 25 nm in this particular case. If it did not rupture it would get into equilibrium at about 8 nm according to the *DLVO* analysis shown in Fig.17. As seen in Figs. 15 and 17, electrostatic attraction between a bubble and treated with hexylamine quartz surface in *DI* water is achieved. It appears now another question – what would be the behavior of wetting film between a bubble and treated with hexylamine quartz in a medium of 0.05 mol/dm³ hexylamine? The inverted Debye length of 0.05 mol/dm³ electrolyte is $1/\kappa$= 1.36 nm, which corresponds to the complete absence of electrostatic interaction until a quite small film thickness (unknown for a while), where an electrostatic attraction should emerge. For better clearness, comparative graphics of draining wetting films are presented with the same radii between the bubble and modified quartz surface in *DI* water and 0.05 mol/dm³ hexylamine in Fig. 17. The surface potential of the quartz surface was considered Ψ_s = – 21.3 mV for the medium *DI* water. It was taken from the experimental measurement of zeta potential of STERILES – MS 45 particles treated preliminary with 0.05 mol/dm³ hexylamine, washed, dried, and added to *DI* water. The surface potential of the quartz surface was considered Ψ_s = – 18.6 mV for the medium 0.05 mol/dm³ hexylamine. It was taken from the experimental measurement of zeta potential of STERILES – MS 45 particles in 0.05 mol/dm³ hexylamine. The surface potential of the air/water interface was considered Ψ_s = 65 mV in both cases.

One can see that the wetting film on modified with hexylamine quartz in *DI* water drains significantly faster than the wetting film on quartz in 0.05 mol/dm³ hexylamine. This is not surprising,
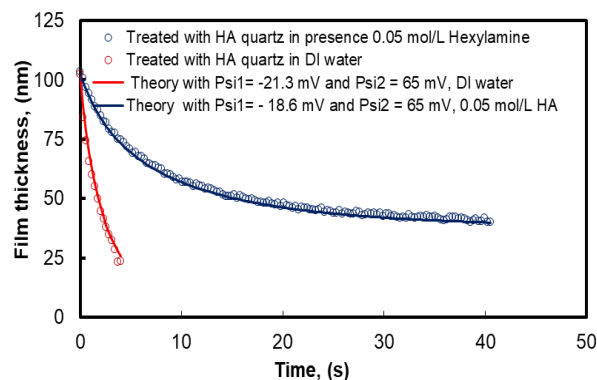
Fig. 17. Wetting film thickness versus time on modified with hexylamine (HA) quartz in *DI* water and in 0.05 mol/dm³ hexylamine
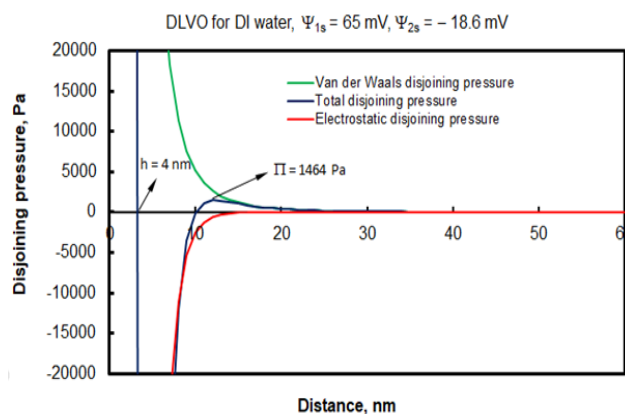
Fig. 18. Electrostatic, van der Waals and total disjoining pressure between a bubble and a treated with hexylamine quartz surface in 0.05 mol/dm³ hexylamine

because the electrostatic attraction in *DI* water is strong due to the very diluted electrolyte concentration. The two surfaces of the wetting film attract each other from a long distance as far as the inverted Debye length for this particular case is $1/\kappa$ = 196.55 nm. On the contrary, in the case of wetting films on quartz in 0.05 mol/dm³ hexylamine, the inverted Debye length is $1/\kappa$ = 1.36 nm. Therefore, the electrostatic attraction is screened and as consequence, the wetting film is subjected only to the capillary pressure and its response – the hydrodynamic resistance at the higher thickness and van der Waals repulsion at thickness smaller than 20 nm and electrostatic attraction at a very small thickness (unknown for a while). Therefore, one can see that the wetting film in a medium of 0.05 mol/dm³ hexylamine drains significantly slower than in the medium of *DI* water. One can have an impression that it gets into equilibrium, but this is only at first glance due to the very slow drainage at a thickness below 50 nm. The *DLVO* analysis for this particular case is more difficult because the inverted Debye length ($1/\kappa$ = 1.36 nm) is compatible with the length of the charging $C_6H_{13}NH_4^+$ ions (L ≈ 0.88 nm). In such a situation the electrical double layer (*EDL*) is not well-formed (Dukhin and Goetz 2010). Therefore, the classical Poisson-Boltzmann equation operating with dot charges fails here (Outhwaite and Bhuiyan 2021). Instead charged particles with real sizes should be considered. A basic difference with the classical model is that the Debye constant is corrected:

$$\kappa = \kappa_0 \, exp(2\kappa_0 L), \kappa_0 = \sqrt{\frac{2F^2 c}{\varepsilon\varepsilon_0 RT}} \qquad (22)$$

As seen in Fig. 18, the potential barrier of Π = 1466 Pa between the particle and the bubble, which cannot be overcome within the interferometric experiment (P_c = 32 Pa) but can be overcome within the flotation experiment, at which stochastic turbulent force pushes the bubbles and the particles toward each other during their collisions. The stronger the turbulence the larger the amount of bubble–particle pairs caught in the potential well. Fortunately, the flotation experiments with a Hallimond tube and Denver flotation cell confirmed the *DLVO* analysis.

Shown in Table 1 are the contact angles, the average thickness of film rupture, and the average lifetime of the wetting films from *DI* water on intrinsic and treated with hexylamine quartz.

Table 1. Contact angles, an average thickness of film rupture, and an average lifetime of the wetting films from *DI* water on intrinsic and treated with hexylamine quartz

Mineral	Average contact angle (º)	Average thickness of film rupture (nm)	Average lifetime of the wetting film (sec)
Quartz	27.40 ± 7.4	No rupturing	Many hours
Modified with HA quartz	54.50 ± 5.2	65 ± 52	8.6 ± 7.6

4.2.   Flotation experiments

4.2.1. Denver flotation machine

Fig. 19 shows the recovery of fine silica particles as a function of time. Fig. 19 also presents the recovery of water and the line of best fit for a first-order kinetic model commonly used to model flotation data. The first-order kinetic model fitted the data well. The maximum recovery based on the model was found to be 90.4%. It is important to comment on the entrainment of particles to comment on the collecting ability of hexylamine. Fine particles are known to be prone to entrainment and in such a case the recovery is not chemically selective (Wang, Peng et al. 2015). The entrainment of particles is the result of a net flow of water containing suspended solids. A degree of entrainment, ENT, has been defined as (Wang, Runge et al. 2016).

Wang, Runge et al. (2016) calculated a degree of entrainment for quartz particles finer than 20 μm of 0.4501. A common model for gangue recovery by entrainment for a given size fraction i, $R_{ent,i}$, is given by (Wang, Runge et al. 2016). The estimated recovery by true flotation was obtained by correcting the overall recovery by the recovery by entrainment. Those recoveries are also shown in Fig. 19. The maximum recovery by true flotation was then estimated to be 84.7%, demonstrating the collecting power of hexylamine on fine silica. One can see from the above results, that the electrostatic attraction between bubbles and fine particles helps the latter float well. However, the collector, which it was

chosen (Hexylamine) except making the bubbles and fine particle attract each other electrostatically increase the hydrophobicity of the silica particles to a certain moderate level (see Table 1). Therefore, both the electrostatic attraction + increase of the hydrophobicity gave excellent recovery of the fine particles. To continue this study, it should be asked a question, what will happen if the hydrophobicity of the particles is not increased but only make them attractive with the bubbles electrostatically? For this reason, a special procedure was applied to modify the silica particles, thus shifting their isoelectric point (*IEP*) to pH = 9.2. Therefore, the bubbles will be negatively charged, while the silica particles will be positively charged at pH = 5.8, which is the intrinsic pH of the water in contact with air. Therefore, the surface potential of the silica particles becomes pH-sensitive.
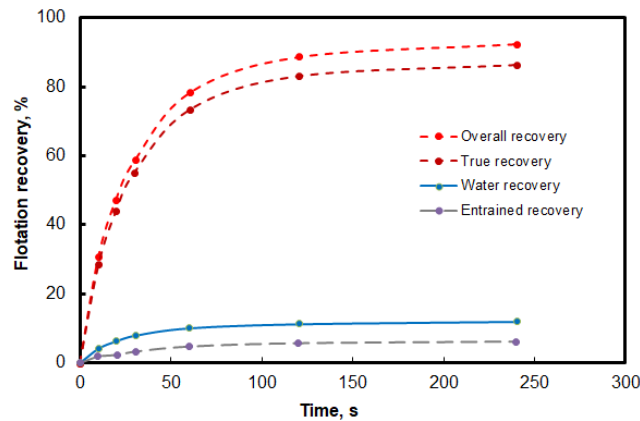

Fig. 19. Recovery of silica fine particles (−20 μm) and water in presence of 0.05 mol/dm³ hexylamine as a function of time. The true and entrained recoveries were estimated based on a degree of entrainment of 0.4501. The experimenyal error is about 2% flotation recovery.

4.2.2. Hallimond tube

A well-known procedure (Anirudhan, Jalajamony et al. 2012) for user-defined adjustment of the isoelectric point of minerals covered with OH groups was applied to fine silica particles. The procedure is described in detail in the literature (Anirudhan, Jalajamony et al. 2012). The idea of the method is to cover the surface of the particles with amino groups. The latter shifts significantly the isoelectric point of the silica particles from pH ≈ 2.5 (Zurita, Carrique et al. 1994) to pH ≈ 9.2. The modification is conducted by means of the chemical reaction between amino-3-methoxy silane (APTMS).

The zeta potential of the intrinsic silica particles versus pH is studied in ref. (Zurita, Carrique et al. 1994), from where one can see that the intrinsic isoelectric point of the silica particles is at pH ≈ 2.5. Fig. 20 shows the zeta potential of modified silica particles and micro-bubbles (Yang, Dabros et al. 2001) versus pH at I = 0.001 mol/dm³. Photo of flotation froth of modified silica particle and in presence of 10
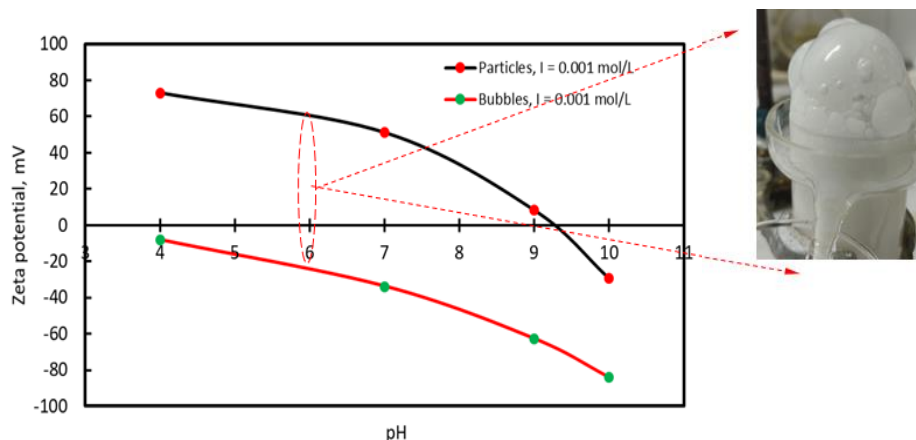

Fig. 20. Zeta potential of modified silica particles and micro-bubbles (Yang, Dabros et al. 2001) versus pH at I = 0.001 mol/dm³. Photo of flotation froth of modified silica particle at 10 ppm MIBC and at pH = 5.8. *IEP* of the particles is at pH = 9.26. The experimental error is about 5 mV

ppm MIBC at pH = 5.8 is shown in Fig. 20 as well. The isoelectric point (*IEP*) of the particles is at pH ≈ 9.2. It is evident in Fig. 20 that the microbubbles and the modified silica particles have opposite signs of the zeta potential (ξ_b = -22 mV, ξ_p = 60 mV) at pH = 5.8. Moreover, the flotation froth shown in the photo of Fig. 20 looks particulate, i.e. it contains a large number of captured particles. The modification of the silica particles does not affect their level of hydrophobicity (CA ≈ 30°). The point here is if such hydrophilic particles can float due only to the electrostatic attraction to the bubbles. The flotation experiments with the Hallimond tube with 1 wt.% suspension of modified fine silica articles (-20 μm) in 10 ppm MIBC and 2 min flotation time gave 47% recovery of the fine silica particles.

The same test with intrinsic fine silica particles gave 11% recovery, which is entrainment recovery. This means that the electrostatic attraction between the bubble and fine silica particles helps to increase their recovery, but a certain increase of the hydrophobicity of the fine particles is needed as well to achieve more than 90% recovery as in the case of the collector hexylamine.

4.3. Bubble-particle attachment time experiments

According to the literature (e.g. ref. (Ahmed and Jameson 1985)), the presence of small bubbles increases the recovery of fine particles. This has been explained by the increase in the flotation collision rate between the fine particles and the bubbles. The analysis is in accord with the literature (Schubert 1999) that the collision rate between the fine particles and the bubbles is sufficiently high to sustain high flotation recovery for a short flotation time if these collisions are efficient. Consequently, the collisions with smaller bubbles are more effective and lead to better capture of the fine particles by the bubbles. Then, the question is why do the smaller bubbles better capture the fine particles than the larger bubbles? The analysis shows that if the fine particles deform the contact area of the bubble during the collision the capillary pressure emerges and gives an additional push to the particles toward the bubble. The capillary pressure can be expressed by the following equation $P_c = 2\sigma/R_b$. The smaller the bubble the larger the capillary pressure and vice versa. The effect of the capillary pressure was studied by means of the bubble-particle attachment timer.

The main objective of the experiments is to explain the bubble-particle- interactions based on the bubble-particle attachment time values. As well-known, the efficiency of flotation is strongly related to the collecting ability of air bubbles. The time required for bubble-particle attachment has a crucial role and is controlled by the physicochemical properties of both bubble and particles.

The flotation experiments were conducted on silica particles (-38 μm + 20 μm) and in presence of 10^{-5} mol/dm³ *DA*H. The bubble–particle attachment time efficiency has been determined with three different radii of the capillary tube: 0.5 mm, 1 mm, and 2 mm. Fig. 21 shows the bubble–particle attachment time efficiency versus the contact time for three different radii of the capillary tubes – 0.5 mm, 1 mm, and 2 mm. It was assumed that the size of the bubble coincided with the size of the capillary tube. The capillary pressure is also given in Fig. 21. One can see that the efficiency is proportional to the
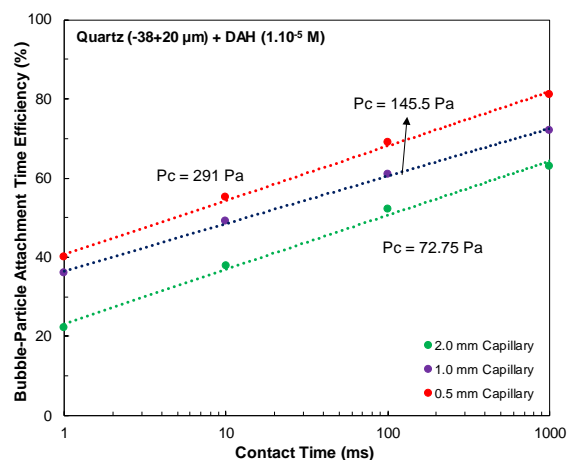

Fig. 21. Bubble – particle attachment efficiency versus contact time on silica particles (-38 μm + 20 μm) and in presence of 10^{-5} mol/dm³ *DA*H and three different radii of the capillary tube. The experimental error is about 2% bubble – particles attachment time efficiency

capillary pressure. Therefore, in the case of fine particles, the collisions with them cause certain deformations in the contact area of the bubbles, thus turning on the capillary pressure.

4.4. Increase of the impeller speed

The increase of the impeller speed increases the energy dissipation in the flotation cell. This causes (i) a decrease in the bubble sizes; (ii) an increase in the hydrodynamic pushing force of the particles; (iii) an increase in the hydrodynamic detachment force of the particles. Therefore, the fine fraction of the feed increases its recovery, but the larger fraction decreases its recovery.

4.5. Increase of the flotation time

As discussed above, the particles with radii in the range of $R_p = 0.2$ μm to $R_p = 2$ μm float but with small flotation rate. For this reason, the increase of the flotation time is a good solution to increase their flotation recovery, but the point is how much the flotation time needs to be increased? In addition, a certain reasonable increase of the flotation time could recover mostly the larger fraction of the fine particles, as far as the flotation rate decreases with the decrease of the particle sizes.

5. Conclusions

The following conclusions were obtained from the theoretical analysis and experimental studies:
1. The rate of collisions between bubbles and fine particles is sufficient at high turbulence to sustain high recovery if the collisions are effective. The problem with the low recovery of the fine particles is the non-effectiveness of most of these collisions.
2. There is a lower thermodynamic limit on the size of the fine hydrophobic ($\theta = 80^o$) particles, bellow which they cannot be captured. This lower size limit depends on the size of the bubbles, with which they collide. It spans in the particle size range of $R_p = 0.16$ μm to $R_p = 0.4$ μm corresponding to bubble size range of $R_b = 50$ μm to $R_b = 1000$ μm. Thus, the fine particles with 0.2 μm $< R_p < 2$ μm float, but with small rate, due to the small exceeding level of the total push force over the maximal resistance force for formation of *TPCL*.
3. Particles with radii larger than 2 μm should have induction time larger than the contact time. Hence, according to the hydrodynamic theory they should be retracted from the bubble, but in reality they float. This can be explained with the occurrence of cavitation of dissolved gases during the bubble – particle collision, causing the formation of gas capillary bridge between the bubble and the particle even at distance in the range of hundreds of nanometers. The intensity of this effect increases with the increase of the size of the particles.
4. Electrostatic attraction between hydrophilic fine silica particles and bubbles can increase their recovery to a certain moderate level (about 47%). Electrostatic attraction between moderately hydrophobized fine silica particles and bubbles can increase significantly their recovery (about 90%).
5. The capillary force during the bubble–particle collision is a powerful factor in the capture of the particles by the bubbles. The smaller bubbles have larger capillary pressure. For this reason, the micro-bubbles contribute to the higher recovery for the fine particles.

Acknowledgments

References

ABRAHAMSON, J., 1975. *Collision rates of small particles in a vigorously turbulent fluid*. Chem. Eng. Sci. 30(11): 1371-1379.

AHMADI, R., D. A. KHODADADI, M. ABDOLLAHY, M. FAN, 2014. *Nano-microbubble flotation of fine, ultrafine chalcopyrite particles*. International Journal of Mining Science, Technology 24(4): 559-566.

AHMED, N., G. J. JAMESON, 1985. *The effect of bubble size on the rate of flotation of fine particles*. Int. J. Miner. Process. 14(3): 195-215.

ALBIJANIC, B., O. OZDEMIR, A. V. NGUYEN, D. BRADSHAW, 2010. *A review of induction, attachment times of wetting thin films between air bubbles, particles, its relevance in the separation of particles by flotation*.Advances in Colloid, Interface Science 159(1): 1-21.

AMELUNXEN, P., R. LADOUCEUR, R. AMELUNXEN, C. YOUNG, 2018. *A phenomenological model of entrainment, froth recovery for interpreting laboratory flotation kinetic tests*. Minerals Engineering 125: 60-65.

ANFRUNS, J. F., J. A. KITCHENER, 1977. "*Rate of capture of small particles in flotation*." Trans. Inst. Min. Metall. (Sect. C) 86: 9-15.

ANIRUDHAN, T. S., S. JALAJAMONY, S. S. SREEKUMARI, 2012. *Adsorption of heavy metal ions from aqueous solutions by amine, carboxylate functionalised bentonites*. Applied Clay Science 65-66: 67-71.

AUSTRALIAN STANDARD (2016). Froth flotation - Basic test (AS 4156.2.1). *Cola preparation: Part 2.1: Higher rank coal.* Sydney, Standards Australia International. AS 4156.2.1: 1-11.

BATCHELOR, G. K. (1956). T*he theory of homogenous turbulence*. Cambridge, Cambridge University Press.

CALGAROTO, S., A. AZEVEDO, J. RUBIO, 2015. *Flotation of quartz particles assisted by nanobubbles*. Int. J. Miner. Process. 137: 64-70.

DAI, Z., D. FORNASIERO, J. RALSTON, 1999. *Particle-bubble attachment in mineral flotation*. J. Colloid Interface Sci. 217(1): 70-76.

DE VIVO, D. G., B. L. KARGER, 1970. *Studies in the flotation of colloidal particulates:effects of aggregation in the flotation process*. Sep. Sci. 5: 145-167.

DOBBY, G. S., J. A. FINCH, 1986. *A model of particle sliding time for flotation size bubbles*. J. Colloid Interface Sci. 109(2): 493-498.

DOBBY, G. S., J. A. FINCH, 1987. *Particle size dependence in flotation derived from a fundamental model of the capture process*. Int. J. Miner. Process. 21(3-4): 241-260.

DUKHIN, A. S., P. J. GOETZ (2010). *Fundamentals of interface, colloid science*. Studies in Interface Science, Elsevier B.V. 24: 21-89.

EXEROWA, D., P. M. KRUGLYAKOV (1997). *Foam, Foam Films: Theory, Experiment, Application*. New York, NY, Marcel Dekker.

FARROKHPAY, S., L. FILIPPOV, D. FORNASIERO, 2020. "*Flotation of Fine Particles: A Review*." Miner. Process. Extr. Metal. Rev.

FENG, D., C. ALDRICH, 1999. *Effect of particle size on flotation performance of complex sulphide ores*. Minerals Engineering 12(7): 721-731.

FLINT, L. R., W. J. HOWARTH, 1971. *Collision efficiency of small particles with spherical air bubbles*. Chem. Eng. Sci. 26(8): 1155-1168.

FORNASIERO, D., L. O. FILIPPOV, 2017. *Innovations in the flotation of fine, coarse particles*. 5th International Conference New Achievements in Materials, Environmental Science, NAMES 2016, Institute of Physics Publishing.

FRIEDLANDER, S. K., 1957. *Behavior of suspended particles in a turbulent fluid*. A.I.Ch.E. Journal 3: 381-385.

GUNGOREN, C., O. OZDEMIR, X. WANG, S. G. OZKAN, J. D. MILLER, 2019. *Effect of ultrasound on bubble-particle interaction in quartz-amine flotation system*. Ultrason. Sonochem. 52: 446-454.

HASSANZADEH, A., M. SAFARI, D. H. HOANG, H. KHOSHDAST, B. ALBIJANIC, P. B. KOWALCZUK, 2022. *Technological assessments on recent developments in fine, coarse particle flotation systems*. Minerals Engineering 180.

KARAKASHEV, S. I., M. FIROUZI, J. WANG, L. ALEXANDROVA, A. V. NGUYEN, 2019. *On the stability of thin films of pure water*. Adv. Colloid Interface Sci. 268: 82-90.

KARAKASHEV, S. I., K. W. STÖCKELHUBER, R. TSEKOV, G. HEINRICH, 2013. *Bubble Rubbing on Solid Surface: Experimental Study*. J Colloid Interface Sci 412: 89-94.

KARAKASHEV, S. I., K. W. STOECKELHUBER, R. TSEKOV, 2011. *Wetting films on chemically patterned surfaces*. J Colloid Interface Sci 363(2): 663-667.

KOMASAWA, I., R. KUBOI, T. OTAKE, 1974. *Fluid, particle motion in turbulent dispersion – I: Measurement of turbulence of liquid by continual pursuit of tracer particle motion*. Chem. Eng. Sci. 29(3): 641-650.

KRALCHEVSKY, P. A., K. D. DANOV, N. D. DENKOV, 2008, *Chemical Physics of Colloid Systems, Interfaces. Handbook of Surface, Colloid Chemistry*. K. S. Birdi, CRC Press: 179-379.

KRALCHEVSKY, P. A., K. D. DANOV, N. D. DENKOV, 2016, *Chemical Physics of Colloid Systems, Interfaces. Handbook of surface, colloid chemistry*. K. S. Birdi. Boca Raron, CRC Press Taylor & Francis Group: 247-413.

LEVICH, V. G. (1962). *Physicochemical Hydrodynamics*. Englewood Cliffs, NJ, Prentice-Hall.

LEVINS, D. M., J. F. GLASTONBURY, 1972. *Particle-liquid hydrodynamics, mass transfer in a stirred vessel. I. Particle-liquid motion*. Trans. Inst. Chem. Eng. 50(1): 32-41.

MANOUCHEHRI, H. R., S. FARROKHPAY, 2016. *Flotation of fine particles – is it the question of power input, bubble size within the cell?* 28th International Mineral Processing Congress, IMPC 2016, Canadian Institute of Mining, Metallurgy, Petroleum.

MEYER, C. J., D. A. DEGLON, 2011. *Particle collision modeling – A review*. Minerals Engineering 24(8): 719-730.

MICHAEL, D. H., P. W. NOREY, 1969. *Particle collision efficiencies for a sphere*. Journal of Fluid Mechanics 37(3): 565-575.

NGUYEN, A. V., H. J. SCHULZE (2004). *Colloidal science of flotation*. New York, Marcel Dekker.

OUTHWAITE, C. W., L. B. BHUIYAN, 2021. *On the modified Poisson-Boltzmann closure for primitive model electrolytes at high concentration*. J. Chem. Phys. 155(1).

OZDEMIR, O., C. KARAGUZEL, A. V. NGUYEN, M. S. CELIK, J. D. MILLER, 2009a. *Contact angle, bubble attachment studies in the flotation of trona, other soluble carbonate salts*. Minerals Engineering 22(2): 168-175.

OZDEMIR, O., S. I. KARAKASHEV, A. V. NGUYEN, J. D. MILLER, 2009b. *Adsorption, surface tension analysis of concentrated alkali halide brine solutions*. Minerals Engineering 22(3): 263-271.

PANCHEV, S. (1971). *Random Functions, Turbulence*, Elsevier Ltd.

PEASE, J. D., D. C. CURRY, M. F. YOUNG, 2005. *Designing flotation circuits for high fines recovery*. Centenary of Flotation Symposium, Brisbane, QLD.

PEASE, J. D., M. F. YOUNG, D. CURRY, N. W. JOHNSON, 2010. *Improving fines recovery by grinding finer*. Transactions of the Institutions of Mining, Metallurgy, Section C: Mineral Processing, Extractive Metallurgy 119(4): 216-222.

PHILIPPOFF, W., 1952. *Some dynamic phenomena in flotation*. Trans. Amer. Inst. Min. Enggrs. Min. Engng. 193 (April): 386-390.

PYKE, B., D. FORNASIERO, J. RALSTON, 2003. *Bubble particle heterocoagulation under turbulent conditions*. Journal of Colloid, Interface Science 265(1): 141-151.

RALSTON, J., D. FORNASIERO, S. GRANO, J. DUAN, T. AKROYD, 2007. *Reducing uncertainty in mineral flotation-flotation rate constant prediction for particles in an operating plant ore*. International Journal of Mineral Processing 84(1-4): 89-98.

REAY, D., G. A. RATCLIFF, 1973. *Removal of fine particles from water by dispersed air flotation. Effects of bubble size, particle size on collection efficiency*. Can. J. Chem. Eng. 51(2): 178-185.

REAY, D., G. A. RATCLIFF, 1975. *Experimental testing of the hydrodynamic collision model of fine particle flotation*. Can. J. Chem. Eng. 53(5): 481-486.

RULYOV, N. N., 2001. *Turbulent microflotation: Theory, experiment*. Coll. Surf. A 192(1-3): 73-91.

RULYOV, N. N., N. K. TUSSUPBAYEV, O. V. KRAVTCHENCO, 2015. *Combined microflotation of fine quartz*. Transactions of the Institutions of Mining, Metallurgy, Section C: Mineral Processing, Extractive Metallurgy 124(4): 217-223.

SAFFMAN, P. G., J. S. TURNER, 1956. *On the collision of drops in turbulent clouds*. J. Fluid Mech. 1(1): 16-30.

SCHELUDKO, A., B. V. TOSHEV, D. T. BOJADJIEV, 1976. *Attachment of particles to a liquid surface (capillary theory of flotation)*. J. Chem. Soc., Faraday Trans. 1 72(12): 2815-2828.

SCHUBERT, H., 1999. *On the turbulence-controlled microprocesses in flotation machines*. Int. J. Miner. Process. 56(1-4): 257-276.

SCHUBERT, H., E. HEIDENREICH, F. LIEPE, T. NEESSE (1990). Mechanische Verfahrenstechnik. Leipzig, Deutscher Verlag für Grundstoffindustrie.

SLAVCHOV, R., B. RADOEV, STOCKELHUBER, K.W., 2005. *Equilibrium profile, rupture of wetting film on heterogeneous substrates*. Coll. Surf. A 261(1-3): 135-140.

SUTHERLAND, K., 1948. *The physical chemistry of flotation XI. Kinetics of the flotation process*. J. Phys. Chem. 52: 394-425.

TRAHAR, W. J., 1976. *The selective flotation of galena from sphalerite with special reference to the effects of particle size*. Int. J. Miner. Process. 3(2): 151-166.

TRAHAR, W. J., 1981. *A rational interpretation of the role of particle size in flotation*. Int. J. Miner. Process. 8(4): 289-327.

VON SMOLUCHOWSKI, M., 1917. "*Versucheiner Mathematischen Theorie der Koagulations Kinetic Kolloider Lousungen.*" Z. Phys. Chem. 92: 129-168.

WANG, L., Y. PENG, K. RUNGE, D. J. BRADSHAW, 2015. *A review of entrainment: mechanisms, contributing factors, modelling in flotation*. Minerals Engineering 70: 77-91.

WANG, L., K. RUNGE, Y. PENG, C. VOS, 2016. *An empirical model for the degree of entrainment in froth flotation based on particle size, density*. Minerals Engineering 98: 187-193.

YANG, C., T. DABROS, D. Q. LI, J. CZARNECKI, J. H. MASLIYAH, 2001. *Measurement of the zeta potential of gas bubbles in aqueous solutions by microelectrophoresis method*. J. Colloid Interface Sci. 243(1): 128-135.

YOON, R. H., G. H. LUTTRELL, 1989. *The effect of bubble size on fine particle flotation*. Miner. Proc. Extract. Met. Rev. 5: 101-122.

ZURITA, L., F. CARRIQUE, A. V. DELGADO, 1994. *yangThe primary electroviscous effect in silica suspensions. Ionic strength, pH effects*. Coll. Surf. A 92(1-2): 23-28.